HHS Public Access

Author manuscript

Science. Author manuscript; available in PMC 2016 October 01.

Published in final edited form as:

Science. 2016 April 1; 352(6281): 91–95. doi:10.1126/science.aad0467.

A long noncoding RNA associated with susceptibility to celiac disease

Ainara Castellanos-Rubio[1], **Nora Fernandez-Jimenez**[2], **Radomir Kratchmarov**[1], **Xiaobing Luo**[3], **Govind Bhagat**[4,5], **Peter H. R. Green**[5], **Robert Schneider**[6], **Megerditch Kiledjian**[3], **Jose Ramon Bilbao**[2], and **Sankar Ghosh**[1,*]

[1]Department of Microbiology and Immunology, Columbia University, College of Physicians and Surgeons, New York, NY 10032, USA

[2]Department of Genetics, Physical Anthropology, and Animal Physiology, University of the Basque Country (UPV-EHU), BioCruces Research Institute, Leioa 48940, Basque Country, Spain

[3]Department of Pathology and Cell Biology, Columbia University, College of Physicians and Surgeons, New York, NY 10032, USA

[4]Center for Celiac Disease, Department of Medicine, Columbia University, College of Physicians and Surgeons, New York, NY 10032, USA

[5]Alexandria Center for Life Sciences, New York University School of Medicine, New York, NY 10016, USA

[6]Department of Cell Biology and Neuroscience, Rutgers, The State University of New Jersey, Piscataway, NJ 08854, USA

Abstract

Recent studies have implicated long noncoding RNAs (lncRNAs) as regulators of many important biological processes. Here we report on the identification and characterization of a lncRNA, lnc13, that harbors a celiac disease–associated haplotype block and represses expression of certain inflammatory genes under homeostatic conditions. Lnc13 regulates gene expression by binding to hnRNPD, a member of a family of ubiquitously expressed heterogeneous nuclear ribonucleoproteins (hnRNPs). Upon stimulation, lnc13 levels are reduced, thereby allowing increased expression of the repressed genes. Lnc13 levels are significantly decreased in small intestinal biopsy samples from patients with celiac disease, which suggests that down-regulation of lnc13 may contribute to the inflammation seen in this disease. Furthermore, the lnc13 disease-associated variant binds hnRNPD less efficiently than its wild-type counterpart, thus helping to explain how these single-nucleotide polymorphisms contribute to celiac disease.

*Corresponding author. sg2715@columbia.edu.

SUPPLEMENTARY MATERIALS

www.sciencemag.org/content/352/6281/91/suppl/DC1)

Materials and Methods

Supplementary Text

Figs. S1 to S9

Tables S1 to S4

References (*31*, *32*)

Roughly 80% of the phenotype-related loci identified by genome-wide association studies (GWAS) of many human diseases map to noncoding genome regions. Long noncoding RNAs (lncRNAs) represent a large portion of noncoding regions across the genome (1); however, the link between the GWAS phenotype–related loci on lncRNA expression or function—and the implications for disease—remain uncharacterized (2, 3). Celiac disease (CeD) is a chronic, immune-mediated intestinal disorder that is caused by intolerance to ingested gluten and develops in genetically susceptible individuals (4, 5). Recent studies have revealed 39 non– human lymphocyte antigen regions associated with a risk of CeD development, including many in noncoding regions (6–8).

Among the 14 CeD-associated intergenic single-nucleotide polymorphisms (SNPs) identified by GWAS (table S1) (9), rs917997 is 1.5 kb apart from the 3′ end of the *IL18RAP* coding gene in chromosome 2. This region harbors a total of five other CeD-associated SNPs that are transmitted with rs917997 as a haplotype block. No transcript had been mapped to this region in the human genome, although in the positionally equivalent conserved region in mouse, a gene (lnc13) encoding a 2.8-kb transcript has been classified as noncoding, which partly sense-overlaps with the *Il18rap* gene (10) (fig. S1A). Using 5′ and 3′ rapid amplification of cDNA ends, we defined the ends of mouse lnc13, confirming that although the 5′ end of lnc13 overlaps with the 3′ end of Il18rap, the two RNAs are independent (fig. S1B). Polymerase chain reaction (PCR) products generated using PCR primer pairs located along the Il18rap and lnc13 cDNAs (fig. S1C), as well as Northern blot analysis (fig. S1D), further demonstrate that Il18rap and lnc13 are independent transcripts.

As this region is highly conserved between mice and humans (66.5% identity by TransMap alignment, 59% identity by pairwise alignment) (figs. S1B and S2A), we hypothesized that an equivalent lncRNA might exist in the human genome. Intestinal cell RNA sequencing (RNA-seq), histone modification, chromatin signature, and deoxyribonuclease hypersensitivity site (DHS) data, together with RNA-seq signals in different tissues (11), support the presence of an expressed transcript in this region (fig. S2, A and B). Although the exact ends of the human lncRNA remain to be determined, we confirmed the existence of a DHS, which typically denotes a regulatory region such as an active promoter, close to the predicted 5′ end of the human lncRNA (fig. S3A). DHSs were shown to precede both the *IL18RAP* gene and the *lnc13* gene, supporting their independent expression (fig. S3A). Expression of processed, polyadenylated, and capped human lnc13 was confirmed in the U937 myeloid cell line (fig. S3B), where lnc13 is expressed at a low level of ~10 molecules per cell (fig. S3C), similar to other lncRNAs (12, 13). Moreover, RNA in situ hybridization of intestinal paraffin-embedded sections using RNAscope technology (14) confirmed expression of human lnc13 (Fig. 1A).

Differential expression of lnc13 in different human tissues indicates a possible tissue-specific role (fig. S3D). As our main focus was the intestinal epithelia, given its role in CeD, we examined the presence of the lnc13 transcript in situ in the lamina propria (Fig. 1A) and whole-villi sections of small intestinal biopsy samples (fig. S4A). Biopsies from CeD patients appeared to have substantially lower amounts of lnc13 compared with controls (Fig. 1A and fig. S4A). Quantitation of the decrease of lnc13 in intestinal biopsies of patients with CeD revealed that lnc13 was significantly down-regulated in tissues from patients compared

with healthy controls (Fig. 1B). In contrast, the expression of the overlapping *IL18RAP* coding gene was increased in patient samples (fig. S4B). Both lamina propria lymphocytes (LPLs) and intraepithelial lymphocytes from the small intestine express lnc13, but the decreased level was observed only in the LPL fraction, pointing to a cell type–specific regulation.

We found that the subcellular localization of lnc13 is primarily nuclear in both mouse and human macrophages (fig. S4, C and D). In situ hybridization on small intestinal biopsies also showed nuclear localization of lnc13 in the mononuclear cells of the lamina propria (fig. S4E). Together, the nuclear localization, the poor Kozak consensus sequence in the predicted open reading frame, and the absence of Pfam domains as assessed by the ATGpr (15) and European Molecular Biology Laboratory–European Bioinformatics Institute InterPro prediction programs (16) strongly suggested that lnc13 is unlikely to encode a protein product.

To further characterize lnc13, we stimulated mouse bone marrow–derived macrophages (BMDMs) with lipopolysaccharide (LPS) to mimic an inflammatory environment, as evidenced by the accompanying increase in interleukin-6 (IL-6) (Fig. 1C). Consistent with observations in CeD patients, the level of lnc13 decreased significantly upon LPS stimulation (Fig. 1C and fig. S5A), whereas Il18rap levels showed a transient increase (fig. S5A). Similar results were seen in immortalized bone marrow–derived mouse macrophages (iBMMs) and monocytic cells from the human U937 line (fig. S5, B and C). The LPS-induced decrease of lnc13 is dependent on Myd88 and NF-κB (Fig. 1D and fig. S5, D and E), consistent with the observation that NF-κB is constitutively active in the mucosa of patients with CeD (4). The lack of Myd88 did not affect Il18rap induction but does affect IL-12 (Fig. 1D and fig. S5F). In the absence of NF-κB signaling (Fig. 1D and fig. S5, D and E), we observed an increase in lnc13 expression, which suggests that lnc13 is continuously transcribed as a stable lncRNA (fig. S5G) that is degraded by a pathway dependent on NF-κB signaling.

We compared expression changes of lnc13 with those of 92 protein-coding genes with established inflammatory roles. After LPS stimulation, differentially expressed genes were grouped by their temporal expression pattern (17) (table S2). The expression pattern of the *Traf2*, *Stat1*, *Stat3*, *Tnfsf10*, *Il2ra*, *Ccl12*, *Myd88*, *Csf3*, and *Il1ra* genes inversely correlated with changes in lnc13 (Fig. 2A). Expression of four of these genes (*TRAF2*, *STAT1*, *IL1RA*, and *MYD88*) was significantly increased in biopsies from CeD patients, which suggests that lnc13 levels affect this subset of inflammatory genes (Fig. 2B). Increased levels of lnc13 reduced the expression of the predicted targets, as listed above (Fig. 2C), whereas reduction of lnc13 had the opposite effect (Fig. 2D and fig. S5, H and I), demonstrating a link between lnc13 and the target genes. *IL-15* and *Il18rap* (Fig. 2, C and D, and fig. S5, I and J), which have been associated with CeD pathogenesis (18, 19), did not show significant expression changes upon alteration of lnc13 levels, suggesting that lnc13 affects the expression of a certain subset, but not all the genes that have been implicated in CeD pathogenesis.

We observed that de novo transcription and protein synthesis are involved in the reduction of lnc13 observed in LPS-treated macrophages and CeD biopsies (fig. S6A). The high stability

of lnc13 (fig. S5G) points to a posttranscriptional regulation of this lncRNA. Given the involvement of NF-κB (fig. S5E) and MyD88 (Fig. 1F and fig. S5D) in lnc13 regulation, we hypothesized that LPS-induced activation of NF-κB, through a MyD88-dependent pathway, leads to synthesis of a protein that is responsible and necessary for the reduction of lnc13 RNA. Decapping enzymes, which destabilize capped mRNAs and lncRNAs, have been described to regulate lncRNA levels (20). The expression pattern of decapping protein 2 (Dcp2) was inversely correlated with the level of lnc13 in LPS-stimulated iBMMs (Fig. 3A and fig. S5B) and BMDMs (Fig. 1C and fig. S6B). An increase of total (fig. S6, C and D) and nuclear Dcp2 (Fig. 3B and fig. S6E) after LPS stimulation in mouse and human macrophages was also observed. Furthermore, biopsies of CeD patients showed increased DCP2 expression (Fig. 3C) and relatively higher levels of nuclear Dcp2 as compared with controls (Fig. 3D). iBMMs and BMDMs from Dcp2 hypomorphic knockout (KO) mice (21) stimulated with LPS do not show lnc13 down-regulation (Fig. 3E and fig. S6F), and accumulation of the lnc13 transcript was seen after LPS stimulation in KO mice, strongly suggesting that Dcp2 recognizes lnc13 and causes its degradation. The same pattern was observed when we used human cell lines mutant for the Dcp2 catalytic domain or Dcp2 KO (fig. S6G). Dcp2 functions by binding RNA to recognize the cap for hydrolysis (22). Structural features at the 5′ end of RNA transcripts are known to be essential for Dcp2 targeting (22). We observed that wild-type (WT) lnc13 binds Dcp2 significantly more effectively than the 5′ lnc13 mutants (Fig. 3F), which were predicted to have an altered 5′ loop structure (fig. S6H). These results suggest that recognition of lnc13 by Dcp2 in inflamed tissue contributes to the degradation of lnc13 and the ensuing induction of a subset of inflammatory genes.

Nuclear lnc13 was almost exclusively localized to the chromatin fraction (Fig. 4A), which suggests that it might regulate expression of target genes by recruiting accessory factors to chromatin, similar to the proposed mechanism of other characterized lncRNAs such as lnc-COX2 or HOTAIR (23, 24). The recently described RNA antisense purification (RAP) approach (25), followed by quantitative PCR (QPCR) of specific regions, confirmed the binding of lnc13 to the transcriptional start sites (TSSs) of the target genes (Fig. 4B and fig. S7A). Lnc13-bound proteins were pulled down and subjected to mass spectrometry analysis (fig. S7, B and C, and table S3). One of the major lnc13-binding proteins was an hnRNP (23, 24, 26), namely hnRNPD (also known as AUF1). Mice lacking hnRNPD develop an inflammatory skin disease (27). hnRNPD is able to regulate gene expression through different mechanisms, including interacting with members of the nucleosome-remodeling complex, NuRD, to regulate the epigenetic state of chromatin (28). BMDMs from hnRNPD KO mice did not show any effect on lnc13 down-regulation kinetics (fig. S7D), but expression of lnc13-affected genes in unstimulated and LPS-stimulated cells was increased (Fig. 4C). Human U937 cells also showed increased target gene expression when hnRNPD was knocked down (fig. S7E). Although hnRNPD is expressed as four different isoforms, we found that the p42 isoform bound most efficiently to lnc13. The p42 isoform is also known to be localized to chromatin (29). Chromatin immunoprecipitation (ChIP)–QPCR analysis revealed that hnRNPD binds to the same regions of chromatin as lnc13, but the bound hnRNPD is lost after LPS-stimulated lnc13 degradation (fig. S7F). The chromatin localization of both lnc13 and hnRNPD (Fig. 4A and fig. S7G), together with the enrichment

of both factors in the TSSs of the target genes, further supports the hypothesis that the lnc13-hnRNPD complex functions as a regulator of expression of a subset of inflammatory genes. Interestingly, Hdac1, which is a component of the NuRD remodeling complex, was detected in the hnRNPD p42-lnc13 complex (fig. S7H). Lnc13 was seen to coimmunoprecipitate with Hdac1 in nuclear extracts from mouse and human macrophages (Fig. 4D and fig. S7I). Consistently, ChIP analysis showed enrichment of Hdac1 in the TSSs of lnc13-regulated genes in the steady state, as well as loss of Hdac1 binding after LPS stimulation when lnc13 levels were reduced (fig. S7J). Hdac1 is less efficiently bound to the lnc13 target promoters in cells lacking hnRNPD versus WT cells (Fig. 4E), suggesting that hnRNPD is necessary for Hdac1 to bind the lnc13-regulated promoters. hnRNPD and Hdac1 showed decreased enrichment in the TSSs of the target genes in lnc13 knocked-down (kd) cells compared with those with normal lnc13 levels (Fig. 4F and fig. S7K). The lnc13 kd cells showed higher levels of the target gene expression but no differences in hnRNPD expression (fig. S5J). Taken together, these data suggest that, as described for the binding of Hdac3 by *Xist* lncRNA (30), lnc13 acts as a link between hnRNPD, Hdac1, and chromatin to regulate expression of certain inflammatory genes (fig. S9).

The direct interaction between lnc13 and hnRNPD led us to ask whether the CeD-associated SNP block within lnc13 alters this binding. In fact, the lncRNA structure is predicted to be substantially altered based on the SNP genotype (fig. S8A). Consistent with such a prediction, in vitro–transcribed (IVT) forms of WT and the CeD allele–containing lnc13 reveal dramatically different mobilities on a native agarose gel (fig. S8B). We evaluated the influence of the disease-associated SNPs in the binding between lnc13 and hnRNPD (p42) in human cell lines homozygous for different allelic variants of lnc13: “CC” (WT) and “TT” (disease-associated). Whereas hnRNPD was able to retrieve both forms of lnc13, disease-associated lnc13 was significantly less efficiently bound to the protein in all of the analyzed cell lines (Fig. 4G and fig. S8C). We made the same observation when IVT alleles of lnc13 were used for the pulldown (avoiding the background genomic variation of the different cell lines) (fig. S8D). Experiments using heterozygous cell lines for rs917997 and expressing both alleles confirmed the preferential binding of the C allele (Fig. 4H and fig. S8E). This observation strongly suggests a functional importance for the risk-associated lnc13 haplotype.

The studies presented here identify lnc13 as a previously unrecognized lncRNA that harbors CeD-associated SNPs; demonstrate that lnc13 is degraded by Dcp2 after NF-κB activation; and, most importantly, show that lnc13 is able to regulate the expression of a subset of CeD-associated inflammatory genes through interaction with chromatin and the multifunctional protein hnRNPD (fig. S9). We believe that lnc13 plays a role in the maintenance of intestinal mucosal immune homeostasis and that dysregulation of lnc13 expression and function—as a result of decapping and genetic polymorphisms, respectively—contributes to inflammation in autoimmune disorders such as CeD. Fully deciphering the mechanisms by which lnc13 contributes to the promotion of inflammation may shed light on the mechanisms regulating gene expression and might also reveal previously unidentified targets for use in the diagnosis or treatment of inflammatory diseases such as CeD.

Supplementary Material

Refer to Web version on PubMed Central for supplementary material.

Acknowledgments

We thank S. Gurunathan for assistance with writing the paper and helpful discussions, B. Reizis and C. Schindler for reading the paper and providing helpful comments, and S. Zhang for the mass spectrometry analysis. The data presented here are tabulated in the main paper and the supplementary materials. The sequences reported in this paper have been deposited in the GenBank database (accession number KU712258). This work was supported by a research fellowship from the Basque government (Spain) to A.C.-R. and N.F.-J.; grants from the Basque Department of Health (2011111034) and the Spanish Instituto de Salud Carlos III (PI10/00310) to J.R.B.; NIH grant RO1-GM067005 to M.K.; and NIH grants R37-AI33443, RO1-AI093985, and R01-DK102180 to S.G.

REFERENCES AND NOTES

1. Derrien T, et al. Genome Res. 2012; 22:1775–1789. [PubMed: 22955988]
2. Hindorff LA, et al. Proc Natl Acad Sci USA. 2009; 106:9362–9367. [PubMed: 19474294]
3. Jin G, et al. Carcinogenesis. 2011; 32:1655–1659. [PubMed: 21856995]
4. Fernandez-Jimenez N, et al. Hum Mol Genet. 2014; 23:1298–1310. [PubMed: 24163129]
5. Green PH, Cellier C. N Engl J Med. 2007; 357:1731–1743. [PubMed: 17960014]
6. Dubois PC, et al. Nat Genet. 2010; 42:295–302. [PubMed: 20190752]
7. Trynka G, et al. Nat Genet. 2011; 43:1193–1201. [PubMed: 22057235]
8. van Heel DA, et al. Nat Genet. 2007; 39:827–829. [PubMed: 17558408]
9. Ward LD, Kellis M. Nucleic Acids Res. 2012; 40:D930–D934. [PubMed: 22064851]
10. Carninci P, et al. Science. 2005; 309:1559–1563. [PubMed: 16141072]
11. Skipper M, et al. Nature. 2015; 518:313. [PubMed: 25693561]
12. Yang F, et al. Mol Cell. 2013; 49:1083–1096. [PubMed: 23395002]
13. Cabili MN, et al. Genome Biol. 2015; 16:20. [PubMed: 25630241]
14. Wang F, et al. J Mol Diagn. 2012; 14:22–29. [PubMed: 22166544]
15. Salamov AA, Nishikawa T, Swindells MB. Bioinformatics. 1998; 14:384–390. [PubMed: 9682051]
16. Punta M, et al. Nucleic Acids Res. 2012; 40:D290–D301. [PubMed: 22127870]
17. Ernst J, Bar-Joseph Z. BMC Bioinformatics. 2006; 7:191. [PubMed: 16597342]
18. Abadie V, Discepolo V, Jabri B. Semin Immunopathol. 2012; 34:551–566. [PubMed: 22660791]
19. Periolo N, et al. Cytokine. 2014; 67:44–51. [PubMed: 24680481]
20. Geisler S, Lojek L, Khalil AM, Baker KE. J Coller, Mol Cell. 2012; 45:279–291.
21. Li Y, Song M, Kiledjian M. RNA. 2011; 17:419–428. [PubMed: 21224379]
22. Li Y, Song MG, Kiledjian M. Mol Cell Biol. 2008; 28:939–948. [PubMed: 18039849]
23. Carpenter S, et al. Science. 2013; 341:789–792. [PubMed: 23907535]
24. Khalil AM, et al. Proc Natl Acad Sci USA. 2009; 106:11667–11672. [PubMed: 19571010]
25. Engreitz J, Lander ES, Guttman M. Methods Mol Biol. 2015; 1262:183–197. [PubMed: 25555582]
26. Huarte M, et al. Cell. 2010; 142:409–419. [PubMed: 20673990]
27. Sadri N, Schneider RJ. J Invest Dermatol. 2009; 129:657–670. [PubMed: 18830269]
28. Lee C, et al. Cereb Cortex. 2008; 18:2909–2919. [PubMed: 18413351]
29. Mili S, Shu HJ, Zhao Y, Piñol-Roma S. Mol Cell Biol. 2001; 21:7307–7319. [PubMed: 11585913]
30. McHugh CA, et al. Nature. 2015; 521:232–236. [PubMed: 25915022]

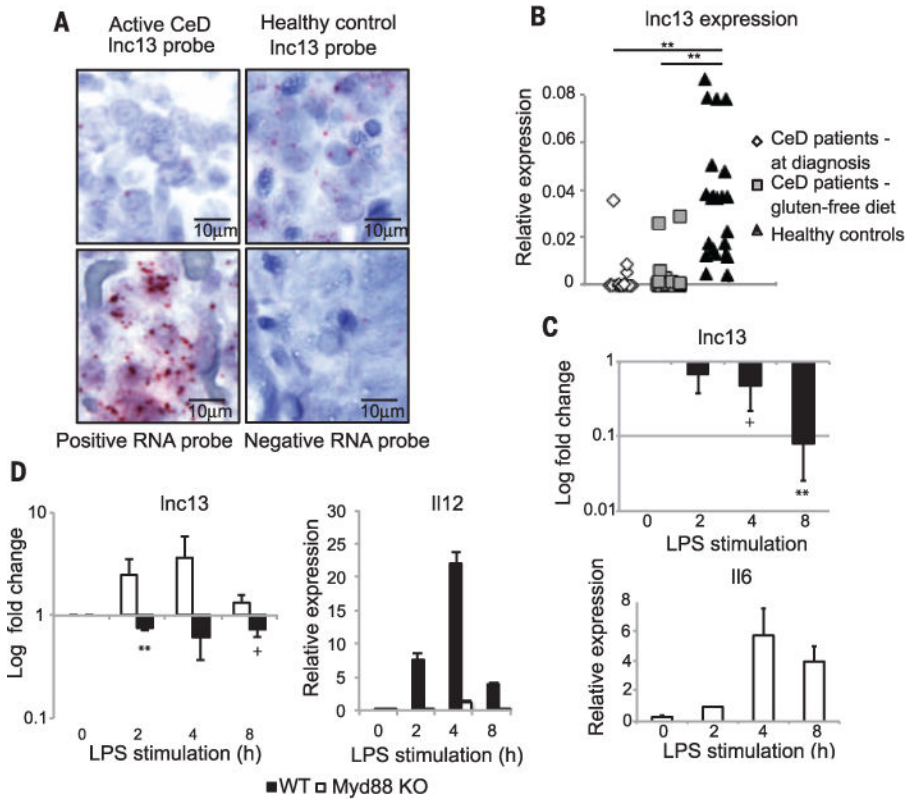

Fig. 1. Lnc13 is an inflammation-dependent lncRNA whose expression is decreased in patients with CeD

(A) Lnc13 expression in human intestinal lamina propria was detected by RNAscope technology. Representative pictures of five samples per condition are shown. Positive control: PPIB; negative control: bacterial dapB. **(B)** Quantitative expression ($2^{-\Delta Ct}$) of human lnc13 using a custom TaqMan expression assay in small intestinal biopsies of control and CeD patients. $^{**}P < 0.01$; unpaired two-sample *t* test. **(C)** Quantitative expression of mouse lnc13 (top) and a stimulation control (IL-6) (bottom) in response to LPS time-course stimulation in primary macrophages. Results represent average and SE (error bars) of three independent experiments. $^{**}P < 0.01$, $^{+}P < 0.1$; unpaired *t* test. **(D)** LPS-induced modulation of lnc13 (left) and IL-12 control (right) levels in WT and Myd88 KO BMDMs extracted from three pairs of mice. Data represent the average and SE of three independent experiments. $^{**}P < 0.01$, $^{+}P < 0.1$; unpaired *t* test.

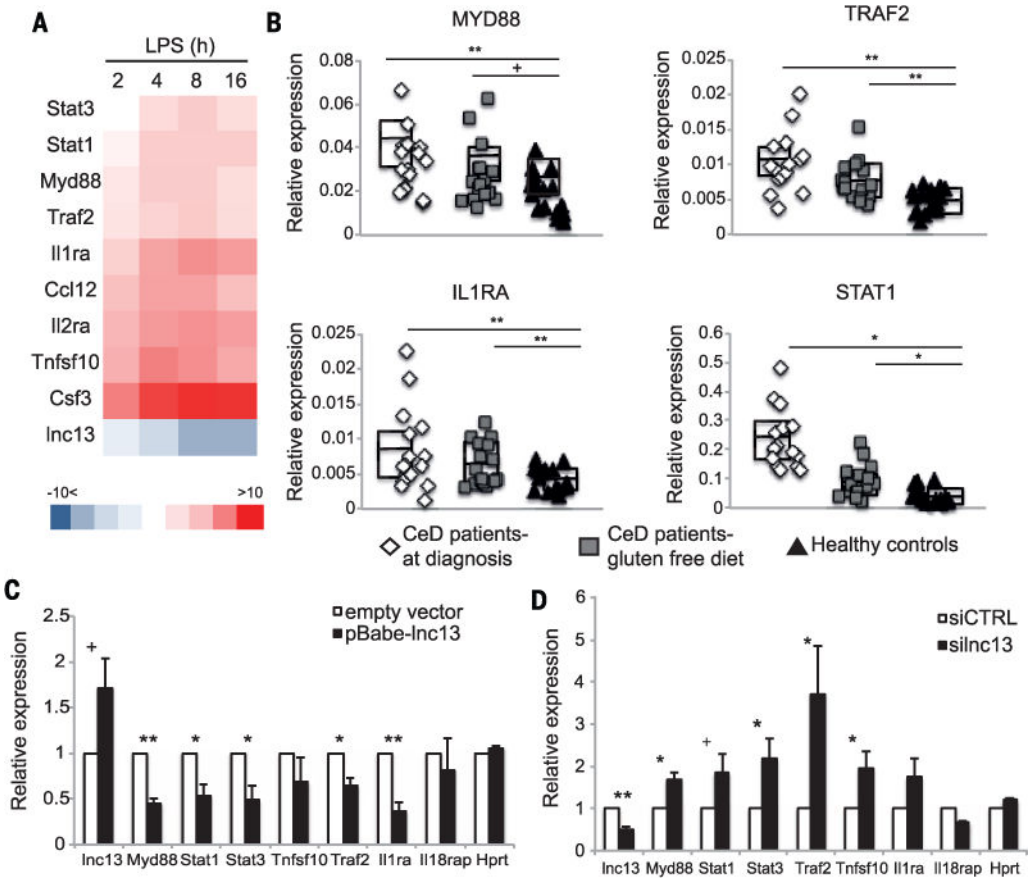

Fig. 2. Lnc13 regulates a subset of CeD-related inflammatory genes

(A) Heat map of the differential expression of a cluster of NF-κB–regulated genes that exhibit expression kinetics highly correlated with lnc13 expression kinetics in response to LPS stimulation (correlation coefficient $R > 0.8$) of BMDMs. **(B)** Celiac disease patients present significantly higher levels of the coexpressed genes indicated in (A), as measured by reverse transcription (RT)–QPCR. Horizontal lines represent average values; white rectangles span the 25th and 75th percentile in each group. $^{**}P < 0.01$, $^{*}P < 0.05$, $^{+}P = 0.05$; unpaired *t* test. **(C)** Immortalized macrophage cell line stably overexpressing lnc13 by a retroviral pBabe-puro vector shows decreased expression of target genes. Data represent the average and SE of four independent experiments. $^{**}P < 0.01$, $^{*}P < 0.05$, $^{+}P \leq 0.1$; unpaired *t* test. **(D)** Immortalized macrophages show lower levels of lnc13 after transfection of custom small interfering RNAs, using the HiPerfect reagent. Lower lnc13 levels result in increased expression of the target genes. Data represent the average and SE of four independent experiments. $^{**}P < 0.01$, $^{*}P < 0.05$, $^{+}P \leq 0.1$; unpaired *t* test.

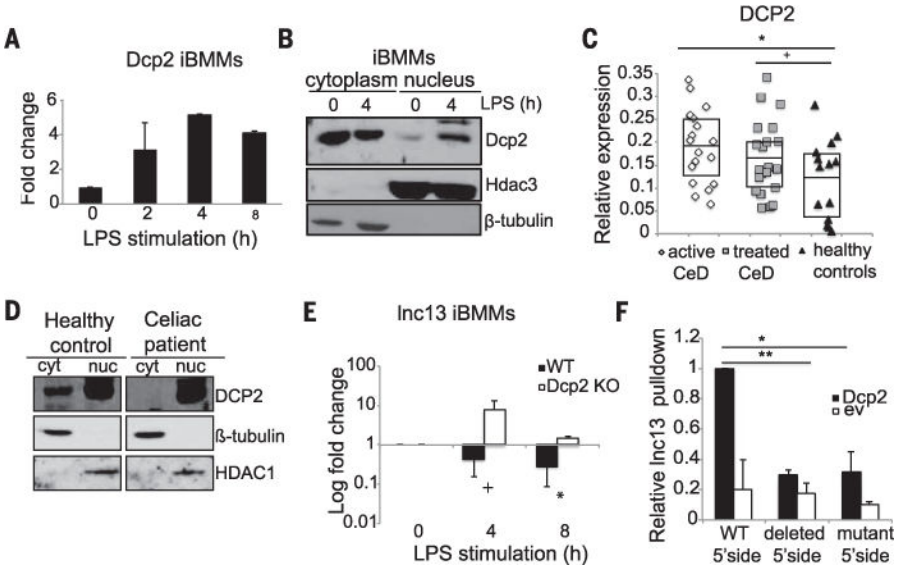

Fig. 3. The Dcp2 decapping enzyme regulates lnc13 levels

(A) Dcp2 expression was measured by RT-QPCR in response to LPS stimulation in iBMMs. Data represent the average and SE of three independent experiments. **(B)** Dcp2 protein levels are increased in the nucleus in response to LPS stimulation of iBMMs. **(C)** Celiac patients show higher levels of Dcp2 expression, as measured by RT-QPCR. Horizontal lines represent average values; white rectangles span the 25th and 75th percentile in each group. $*P < 0.05$, $+P = 0.1$; unpaired *t* test. **(D)** Localization of Dcp2 is mostly nuclear in fractions of intestinal biopsies of patients with CeD compared with healthy controls. This representative figure shows a blot performed on three samples per condition. cyt, cytoplasmic fraction; nuc, nuclear fraction. **(E)** Lnc13 expression pattern after LPS stimulation of WT (black bars) and Dcp2 KO (white bars) iBMMs. Data represent the average and SE of three independent experiments. $*P < 0.05$, $+P < 0.1$; unpaired *t* test. **(F)** WT or 5′ mutant forms of IVT lnc13 were incubated with lysates from cells overexpressing an empty vector (ev) or FLAG-tagged Dcp2. Dcp2 was immunoprecipitated with an antibody to FLAG, and lnc13 levels were quantified by RT-QPCR. The amount of lnc13 in the pulldown is relative to the input of the IVT RNAs and normalized to the full-length WT lnc13. Data represent the average and SE of three independent experiments, $**P < 0.01$, $*P < 0.05$; paired *t* test.

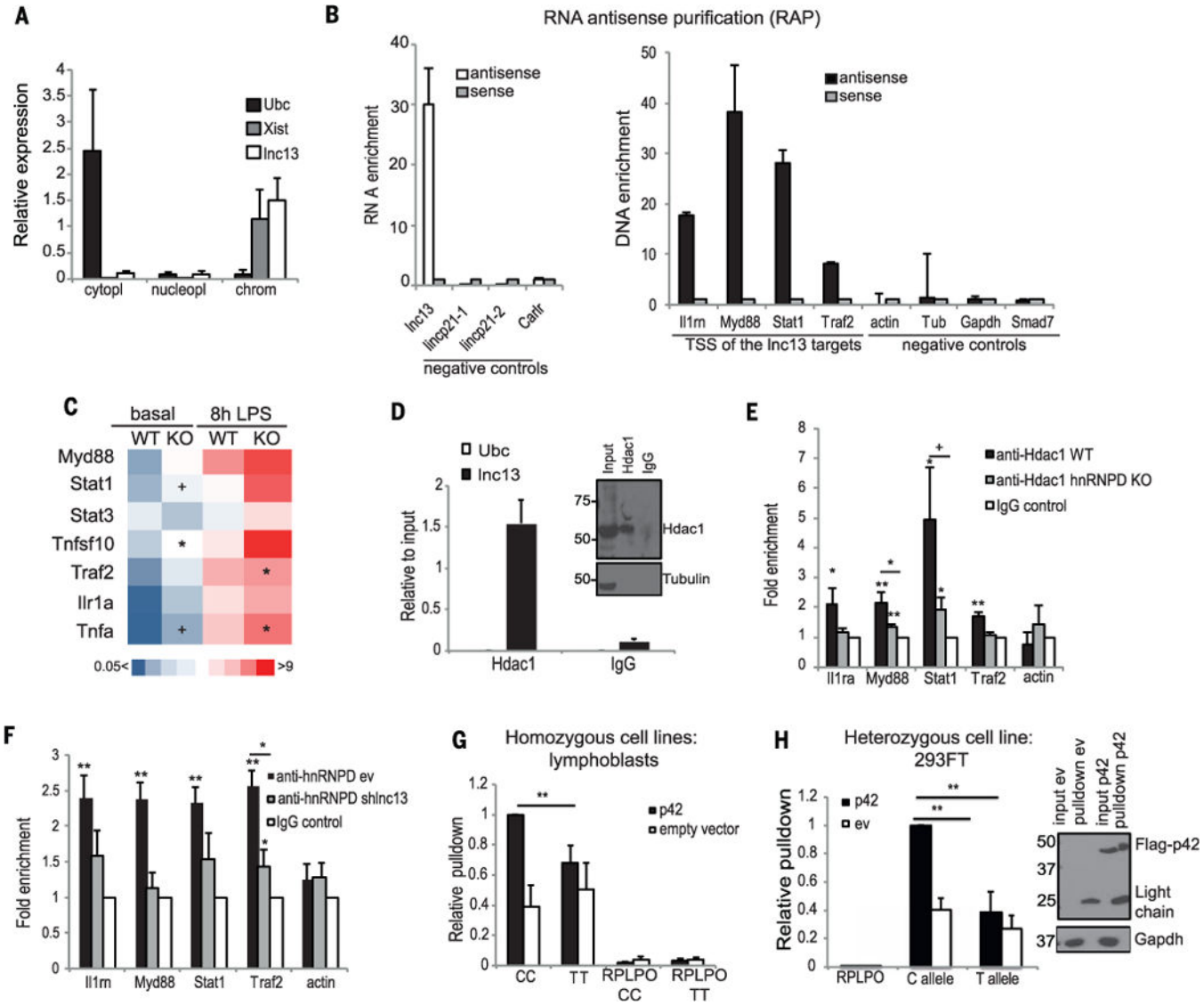

Fig. 4. Lnc13 regulates gene expression by binding to hnRNPD p42 and Hdac1 on chromatin

(A) Determination of lnc13 subcellular localization. Data represent the average and SE of three independent experiments. *Ubc* was used as a cytoplasmic control and *Xist* as a chromatin-associated RNA control. cytopl, cytoplasm; nucleopl, nucleoplasm; chrom, chromatin. **(B)** Lnc13 was purified by the RAP technique, using antisense oligos. Data represent the pulldown percent enrichment of RNA (left) and DNA (right) compared with the sense oligos used as controls. Average and SE of three independent experiments are represented in the graph. **(C)** Expression of lnc13 target genes in BMDMs from hnRNPD KO mice at the basal state and after LPS stimulation. Tumor necrosis factor–α was used as a positive control of overexpression in the KO cells. Data represent the average of three independent experiments. $+P = 0.1$, $*P < 0.05$; unpaired *t* test. **(D)**Interaction between Hdac1 and lnc13 by IP and RT-QPCR. Data represent the average and SE of three independent experiments.IgG, immunoglobulin G. **(E)** ChIP of Hdac1 in WT and hnRNPD KO macrophages. Data represent the average fold enrichment and SE of three independent

experiments. Actin was used as a negative IP control. +$P < 0.1$, *$P < 0.05$, **$P < 0.01$; enrichment based on one-tail z-test; comparison between WT and hnRNPD KO based on two-tailed *t* test. **(F)** ChIP of hnRNPD in macrophages transduced with empty vector (ev) and with a lnc13 short hairpin RNA (sh-lnc13). Data represent the average fold enrichment and SE of five independent experiments. Actin was used as a negative IP control. *$P < 0.05$, **$P < 0.01$; enrichment based on one-tail *z* test; comparison between shlnc13 and ev based on two-tailed *t* test. **(G)** Relative binding affinity of CC- and TT-harboring RNAs to FLAG-hnRNPD, as assessed by FLAG IP and subsequent RT-QPCR. Average and SE data relative to the CC sample are from six independent pulldown experiments. *$P < 0.05$; paired *t* test. **(H)** Quantification of the amount of each allele bound to FLAG-hnRNPD in the heterozygous cell line 293FT (embryonic kidney cells). After IP, each allele was quantified by a dual-color TaqMan assay. Retrieved lnc13 was normalized to input and calculated relative to the C allele. Data represent the average and SD of three independent experiments. RPLPO was used as a negative control. **$P < 0.01$; paired *t* test. Gapdh, glyceraldehyde-3-phosphate dehydrogenase.